# Monitoring Landscape Change in Multi-Use West-central Alberta, Canada using the Disturbance-Inventory Framework

Julia Linke and Gregory J. McDermid

Foothills Facility for Remote Sensing and GIScience, Department of Geography
University of Calgary, 2500 University Drive N.W., Calgary, AB, T2N 1N4, Canada

**Current Address for Corresponding Author**

Julia Linke
Landscape Ecology Laboratory,
Department of Ecology & Evolutionary Biology,
University of Toronto
25 Harbord Street,Toronto, ON, M5S 3G5, Canada
Telephone: +1 (416) 946-7886
Fax: +1 (416) 978-3542
E-mail: julia.linke@utoronto.ca

Submitted for publication in

*Remote Sensing of Environment*

April 30, 2012

(in revised form July 11, 2012)

**Abstract**

Human disturbances are a major driver of biodiversity declines world-wide, and the intensely used Alberta forest landscape is no exception to this trend. Monitoring of such large areas is typically conducted via multi-temporal land-cover maps from remote sensing, but automated and efficient procedures for reliable, operational applications have yet to be fully developed. In an effort to contribute to this need, we developed an innovative approach to landscape monitoring: the disturbance-inventory framework, which is applied for the first time as described here to monitor annual changes in an 8800-km$^2$ multi-use landscape in west-central Alberta, Canada. Using this framework, we (1) report on the spatio-temporal distribution of industrial disturbances such as harvesting cutblocks, oil and gas wells, coal mines, and road/pipelines; and (2) track the associated annual changes in land-cover composition and configuration between 1998 and 2005. To enable spatially explicit analyses within the study area, we divided it into 178, 49km$^2$-square landscape cells. The overall area-based annual rate of change of 0.62% for this multi-use may be considered moderate compared to other regions, where change was mainly shaped by a single use, i.e., forestry. However, the spatially explicit nature of our analysis revealed that the eastern half of the study area is subject to considerably higher rates of change, mainly due to the concurrent appearance of disturbances from forestry and the oil and gas industry. The western half, by contrast, is more restricted by rugged terrain and fewer roads. The average distance to disturbance features across the entire study area decreased from 1500 m to 1200 m over the seven years. Total forest area, mean and largest patch size, and mean shape index all decreased consistently over the same period. The detected rapid change and associated fragmentation call for ongoing monitoring of this and other multi-use landscapes, which could be undertaken using this framework.

## 1. Introduction

Human activities have become the source of much contemporary landscape change, in part by altering the amount, spatial pattern, and character of global vegetation communities (Houghton 1994, Lambien *et al.* 2001, Foley *et al.* 2005). These human-induced modifications have been identified as a major cause of biodiversity decline and species endangerment (Hansen *et al.* 2001, Balmford *et al.* 2003), stimulating a growing emphasis on monitoring programs designed to reveal the consequences of anthropogenic development on natural systems. The public lands that comprise much of Alberta's Rocky Mountain foothills are no exception to this global trend, and are an example of a fast-changing forested landscape that supports intensive use by a variety of resource-extraction industries, including forestry, coal mining, and petroleum development (Schneider *et al.* 2003, Linke *et al.* 2005, 2008). At the same time, this area is host to native wildlife and iconic species, including the threatened woodland caribou (*Rangifer tarandus caribou*) (ASRD/ACA 2010a) and the grizzly bear (*Ursus arctos*), recently also designated as threatened in this Canadian province (ASRD/ACA 2010b). These issues greatly contribute to the monitoring obligations borne by managers and regulators in this landscape (AGBRP 2008) and evoke inquiries regarding the distribution, extent and proximity of industry-related disturbances and their associated changes in landscape structure over time.

Remote sensing has long been considered an essential tool for monitoring landscape change (Skole *et al.* 1997, Kerr and Ostrovsky 2003, Turner *et al.* 2003) but the challenges associated with moving from change detection to landscape monitoring are complex. In essence, landscape monitoring involves the comparison of landscape conditions across two or more dates in time, and may involve the use of landscape pattern analysis (LPA) (O'Neill *et al.* 1988, Li and Wu 2007) to quantify transitions in structural composition (i.e., area of cover-types; e.g., Fry *et* *al.* 2011) and/or configuration (i.e., edge density, patch connectivity; e.g., Southworth *et al.* 2002). While various remote-sensing techniques exist for detecting and analyzing change (Coppin *et al*. 2004, Lu *et al.* 2004, Blaschke 2005, Desclée *et al.* 2006), conventional approaches commonly rely on independently classified land-cover maps (i.e., *post-classification analysis*), often with little attention paid to issues of classification accuracy (Hess 1994, Newton *et al.* 2008) and the propagation of errors (Singh 1989, Mas 2005). *Spurious changes* are differences between maps that are not caused by real changes on the ground, but rather by classification errors arising from differences in atmosphere, illumination, vegetation phenology, soil moisture, satellite-sensor configuration, image-to-ground registration, map-to-map alignment, and classification performance between two or more dates (Yuan and Elvidge 1998, Carmel *et al*. 2001; Mas 2005). While propagation of classification errors were not viewed as a serious hindrance to LPA in early work (e.g., Wickham *et al.* 1997), more recent studies have demonstrated their large and mainly unpredictable impact on landscape pattern indices (Brown *et al.* 2000, Shao *et al.* 2001, Langford *et al.* 2006), calling into question the reliability of nearly every LPA study ever published (Gergel 2006, Langford *et al.* 2006).

While post-classification change analysis may work well under conditions where changes are reported in an aggregated, aspatial manner (Vogelman *et al.* 2001, Ahlqvist 2008), there is a growing need to identify the pattern, nature, and magnitude of change more explicitly (Xian *et al.* 2009), and to incorporate the temporal variability of landscape pattern dynamics into ecological studies (Cushman and McGarigal 2006). As such, we require the development of processing strategies capable of producing consistent, multi-temporal series of land-cover products, thereby enabling reliable and repeatable landscape monitoring (e.g., Gillanders *et al*. 2008, Shao and Wu 2008).

An alternative to post-classification analysis is *map updating*, wherein an existing map product (i.e., *reference map* $T_0$) is updated to a second point in time ($T_n$) through its reclassification only within the regions of identified change between the two dates (Change $T_n$ – $T_0$). This strategy precludes the occurrence of any spurious change outside the areas being updated, thereby increasing the thematic and spatial consistency of map products across the entire monitoring horizon (McDermid *et al.* 2008, Fry *et al.* 2011). Despite these advantages, map updating is not free of challenges. For example, slight spatial mismatches between the boundaries of change regions and existing features in the reference map occur regularly, arising from the fact that it is practically impossible to delineate dynamic objects in a spatially consistent manner across two or more time periods (McDermid *et al.* 2008). These mismatches introduce small, spurious artifacts, such as slivers and gaps, in the updated or backdated maps (McDermid *et al.* 2008), and are similar to those generated from polygon-overlay operations in Geographic Information Systems (GIS) analysis (Goodchild 1978; Chrisman 1989). Despite their small size, these slivers and gaps can seriously distort the rate and direction of change trajectories for landscape pattern indices, thereby compromising their ability to monitor trends over time (Linke *et al.* 2009a).

While accurate, precise, and consistent map-updating of land-cover polygons is undoubtedly best-achieved through human image-interpretation and manual editing (e.g., Loveland *et al.* 2002, Sohl *et al.* 2004, Feranec *et al.* 2007), this is an exceptionally labor-intensive process, and not feasible for monitoring projects extending over large areas and/or frequent time intervals. Automated processing strategies for generating multi-temporal map series that reduce labor costs while maintaining high standards of accuracy and consistency are still highly sought after, and remain “the Holy Grail of change detection” (Loveland *et al.* 2002 p. 1098).

In an effort to contribute towards this goal, we have developed an innovative approach to multi-temporal mapping and landscape monitoring: the *disturbance-inventory (D-I) framework* (Linke *et al.* 2009b, Linke and McDermid 2011). The D-I framework enables the generation of a spatially consistent time series of land-cover maps in a semi-automated, repeatable manner; without the need for manual alterations of the boundaries of change regions. It is designed to account for land-cover conversions specifically related to disturbance events and uses a combination of raster- and vector-operations in a GIS environment to: (1) store, classify, and manipulate *dynamic objects* (i.e., objects that appear, disappear, and/or change thematically over the monitoring horizon); and (2) seamlessly integrate these objects into an existing thematic map. In identifying the need for this research (McDermid *et al*., 2008), demonstrating the issues to be overcome (Linke *et al*. 2009a), and articulating the solution (Linke *et al*., 2009b; Linke and McDermid, 2011), we have developed a foundation for spatially consistent monitoring. Our next goal is to demonstrate the application of the D-I framework in operational monitoring programs, and establish the value of our approach to projects that aim to understand the impacts of human-induced disturbance on our natural landscapes.

The objective of this paper is to present and discuss the results of a multi-temporal monitoring program designed to track changes in the multi-use foothills of west-central Alberta, Canada. Specifically, we describe the spatio-temporal distribution of disturbance features brought about by industrial development, and track the associated annual changes in land-cover pattern for a large, 8800-$km^2$ area between the years 1998 and 2005. In order to make this paper self-contained, we first provide a background summary of the conceptual foundations of the D-I framework. Then, we describe the methods used for the change monitoring in this application, followed by the delivery of the monitoring results. The paper concludes with a discussion of key findings and implications for future monitoring studies.

## 2. The D-I Framework for Multi-temporal Land-cover Mapping

### *2.1 Basic Components, Workflow, and Output Products*

In order to generate a spatially consistent time series of land-cover using the D-I framework, two basic components are needed: (1) a *reference map*; and (2) a *D-I* GIS-vector layer (Figure 1). The reference map consists of a mosaic of non-overlapping map objects, wherein each object is a contiguous area sharing the same land-cover attribute. This map represents land-cover conditions at time $T_0$, and serves as the basis for any projections backward ($T_{-n}$) (i.e., *backdating*) and forward ($T_{+n}$) (i.e., *updating*) through time. The disturbance inventory contains the full collection of dynamic objects observed over the monitoring horizon, wherein each is stored as a unique, discrete entity in a geospatial database, and represents an actual ground feature appearing, disappearing, and/or changing land-cover attribute between any successive time step ($n$) of the monitoring horizon ($T_{-n}$ to $T_{+n}$). Since the actual change agents captured here are generally rooted in natural or anthropogenic disturbances, the dynamic objects are interchangeably referred to as *disturbance features*. These objects can be derived from a variety of bi-temporal change-detection methods, such as, for example, through semi-automated thresholding and segmentation of difference images (e.g., Franklin *et al.* 2001), and/or from digitized GIS layers based on manual photo-interpretation (e.g., Linke *et al.* 2009b).

In order to serve as the means for updating and backdating the reference map, each dynamic object is classified with temporally relevant land-cover attributes for each time step

($LC_n$) of the monitoring horizon, which could be derived in a variety of manners, including standard multi-spectral image classification of the respective images. Using these land-cover attributes, *backdate* and *update* layers are generated by integrating the D-I vector layer into the original reference map ($T_0$), thereby replacing the spatially coinciding land-cover values for each respective instance in time ($T_n$) (Figure 1). Classifying the dynamic objects with attributes, such as time of origin (i.e., disturbance year) and disturbance type, guides and constrains the temporally logical and consistent assignment of the land-cover attributes ($LC_n$) using GIS decision-rules. For example, the attribute 'disturbance type' can imply the spatial overlay order of dynamic features, since disturbance entities are not always mutually exclusive, and can overlap one another in space and time (e.g., a wellsite, ID 6, or a road, ID 7, constructed on top of a forestry cutblock, ID 5 in Figure 1). Storing the dynamic features in a manner that can be referenced in a temporally ascending order – i.e., according to their disturbance year and spatial overlay order – ensures their proper appearance in the backdate/update layers. The time of origin is easily acquired from the bi-temporal change-detection results (i.e., the date when the dynamic feature first appears in the monitoring horizon). Disturbance type may be derived from a combination of spectral, spatial, and contextual information using decision-tree classification approaches (Linke *et al.* 2009b).

It is important to stress that the resulting temporally dynamic series of land-cover maps is not generated by modifying the geometry of the dynamic objects in the disturbance inventory, but rather by changing their land-cover attributes. This allows a map feature to exhibit a variety of dynamics over time, as illustrated in Figure 1, including *appearance* (e.g., new wellsite – object ID 6 corresponding to feature C – first arises in backdated map $T_{-1}$), *disappearance* (e.g., old cutblock – object ID 1 corresponding to feature B – is removed in updated map $T_{+2}$), *persistence* (e.g., old cutblock –object IDs 1, 2, and 3 corresponding to feature B – remains 'shrub' between $T_{-2}$ and in $T_{-1}$), and *succession* (e.g., new cutblock – object IDs 4 and 5 corresponding to feature A – changes from 'barren' to 'herb' stage between backdated map $T_{-1}$ and reference map $T_0$). Natural succession and disturbance events can however also affect the location and shape of a map feature over time, which practically occurs through the gain or loss of its parts and therefore constitutes additional important dynamics such as *feature shrinkage* and *expansion*. Since the D-I framework maintains stable geometries for each dynamic feature over the monitoring horizon, it accomplishes these dynamics by treating each gained or lost part as a unique dynamic object in the inventory. A single map feature can therefore be comprised of several adjacent dynamic objects, each with a different time-of-origin, enabling a feature to *expand* (e.g., new cutblock – ID 4 corresponding to feature A at $T_{-2}$ – expands by $T_{-1}$ due to a change in land-cover value of adjacent dynamic object ID 5 from 'forest' to 'barren') or to *shrink* (e.g., old cutblock – object IDs 1, 2, and 3 corresponding to feature B at $T_{-1}$ – decreases in size by $T_0$ since object ID 2 was not existing in the reference map, and further shrunk by $T_{+1}$ due to the conversion of 'shrub' to 'forest' dynamic object ID 3) over the land-cover map series (Figure 1).

In summary, the D-I framework generates thematically and spatially consistent time series of land-cover maps by: (1) altering the thematic attributes of the reference map *only in areas of change* via spatially stable dynamic objects; and (2) maintaining all other areas of the map in their original condition (i.e., *static objects*) over the entire monitoring horizon. While this approach does nothing to fix classification errors that may exist in the original reference map, it limits the introduction of new errors that would then propagate through the rest of the analysis. As a result, the map series serves as an appropriate basis for spatially explicit multi-temporal *LPA* of the evolving patch mosaic. While used as a basic component for multi-temporal map generation, the disturbance inventory corresponds to the entire extent of change observed over the monitoring horizon, and hence constitutes a product in and of itself; enabling the multi-temporal analysis of all detected disturbances.

* Figure 1 here *

### *2.2 Framework Criteria and Conditions for Seamless Integration of Dynamic Objects*

The quality of the multi-temporal map series generated by the D-I framework is a function of the accuracy and consistency of both the reference map and the disturbance inventory. Since any spatial or thematic errors in the reference map, outside the regions of change will remain unaltered throughout the entire time series, they will not affect landscape change analyses performed on the generated map series (Linke *et al.* 2009a). However, they can create systematic under- or over-estimates of land-cover composition or configuration, and should therefore be corrected in advance if the reference map is judged to be of sub-standard quality. Of greater concern are errors within the disturbance inventory, since these can reduce the reliability of the final map series for monitoring purposes, causing under- and/or over-estimates of the area changed. The selection of minimum mapping units, appropriate for the types of dynamic objects to be detected from the source imagery, in combination with robust change-detection methods (Sundaresan *et al.* 2007, Walter *et al.* 2004), are general criteria to be followed and are also important for this framework.

Rigorous application of robust change-detection algorithms will however not preclude spatial mismatches between the boundaries of dynamic objects and those of objects existing in the original reference map, hereby hindering seamless integration of the dynamic objects during the backdating and updating process, and therefore leading to spurious artifacts in the final maps.

In cases when the boundary of a dynamic object *undershoots* that of a spatially coinciding object (mismatches *b*, *c*, and *d*, Figure 2) or adjacent object (mismatches *e*, Figure 2) of the reference map, spurious *slivers* or *gaps* can arise in the backdated or updated map products. In cases of *overshoots* of a spatially coinciding object (mismatch *a*, Figure 2) or an adjacent object (mismatch *f*, Figure 2) of the reference map, spurious *stretches* or *encroachments* can respectively manifest themselves in the final map products. These artifacts are in essence *intersect objects* created by the mismatch between vector outlines of the dynamic objects and those of the objects from the reference map (Figure 2).

In order to suppress such small-but-significant artifacts (McDermid *et al.* 2008, Linke *et al.* 2009a), the boundaries of the dynamic objects need to be *conditioned* before the actual map updating or backdating can be performed. Two assumptions apply for such conditioning: (1) the object boundaries of the reference map should be treated as correct, and dynamic-object boundaries must adhere to them; and (2) all intersect objects narrower than an operator-specified minimum mapping width (MMW) are assumed to originate from boundary mismatches and are therefore treated as spurious (Linke and McDermid 2011). This assumption consequently also determines the narrowest width for which a dynamic object will be detected. The MMW can be determined through a visual inspection of boundary mismatches and the respective image pairs from which the dynamic objects were derived, thereby balancing the omission of small dynamic objects (in case of a larger MMW) against the commission of spurious change artifacts (in case of a smaller MMW). The value of the MMW is expected to be no greater than that published for standard photo-interpretation guidelines (Loveland *et al.* 2002), and generally ranges between two and four pixels (e.g., Linke *et al.* 2009). The actual boundary-conditioning can be accomplished using automated GIS tools by first creating a new temporary vector database of all *intersect objects*, created by first intersecting the dynamic-objects layer with the vector outlines of the reference map, and then trimming and expanding the dynamic objects with these intersect objects, following specific proximity and MMW constraints (e.g., Linke *et al*. 2009). Applied properly, these boundary-conditioning rules enable the seamless integration of dynamic objects derived from either automated or manual approaches.

* Figure 2 here *

## 3. Landscape Monitoring in West-central Alberta, Canada: Materials and Methods

### *3.1 Study Area*

The 8721-km$^2$ study area is located in the west-central core of the Alberta foothills of western Canada (Figure 3), just east of Jasper National Park. The area is situated south of Hinton and is occupied primarily by closed-canopied, pure- and mixed-coniferous (*Picea glauca*, *Picea engelmanii*, *Pinus contorta*, *Abies lasiocarpa)* and deciduous (*Populus* spp.) forests (Strong 1992, Beckingham *et al.* 1996). The region encompasses an elevation gain from about 1000m on the east, to about 2400m along its western border. Six main types of disturbances dominate and shape the study area. These are: (1) cutblocks created by forest clear-cutting; (2) surface or open-pit mines arising from coal extraction; (3) wellsites, which consist typically of a gas well surrounded by a ~1-ha patch of cleared terrain; (4) pipelines, for transporting oil and gas along ~30m-wide herbaceous corridors; (5) roads, ranging in size from one-lane dirt or gravel roads to multi-lane highways; and (6) burns from fires. Five-meter-wide seismic lines cut for oil and gas exploration also form part of this landscape (Linke *et al.* 2008), but are not monitored in this study, since they are not discernible from the medium-resolution Landsat imagery used to construct the time series (described below).

### *3.2 Data Sets*

Annual land-cover maps were generated using the D-I framework for the years between 1998 and 2005 (Figure 3). The reference map used for this process consisted of an object-based map depicting 10 basic land-cover classes (upland trees, wetland trees, upland herb, wetland herb, shrubs, barren land, water, snow/ice, cloud, shadow) for the summer of 2003 with an overall accuracy of 91.8% (McDermid 2005). The D-I vector layer was created using annual Landsat Thematic Mapper (TM) and Enhanced Thematic Mapper Plus (ETM+) summer images (path 45/row 23). This disturbance inventory stored vector entities depicting the unique disturbance objects that arose or changed between 1998 and 2005, and recorded the year of origin, disturbance type, and land-cover class for each annual time step as attributes (Figure 3). Objects with a year-of-origin of 1998 represented disturbance features that pre-dated the monitoring horizon, and hence together represented the cumulative collection of *existing* disturbance objects up to 1998. All other objects, with years-of-origin between 1999 and 2005, constituted *annual* disturbances that originated in each respective year. Areal disturbance features (i.e., cutblocks, mines, and natural fires) were derived through automatic segmentation of manually thresholded, bi-temporal difference layers using the Enhanced Wetness Difference Index method of change detection (Franklin *et al.* 2001). Manual delineation of the same imagery was used for the linear- (i.e., roads and pipelines) and point-based (i.e., well sites) disturbance features. All detected disturbances represented vegetation-replacing changes, transitioning primarily from forest cover type to barren or herbaceous types at the time of origin, depending on the type of disturbance. The disturbance inventory was assessed as having overall accuracies of 100% for change detection, 98% for disturbance-type classification, and 80% for land-cover classification (Linke *et al.* 2009b). A MMW of 60m for adjacent and 120m for coinciding features was applied for boundary conditioning of the disturbance objects; however, roads, pipelines and wellsites were exempt from the MMW constraint, since they were absent from the reference map and originated from manually verified delineation (Linke *et al.* 2009b).

* Figure 3 here *

### *3.3 Analysis of Disturbance Features and Land-cover Pattern*

We calculated annual rates of change across the study area as an indication of overall multi-temporal changes occurring in this selected Foothills landscape. With the disturbance inventory representing all vegetation-replacing changes occurring of the study area, annual rates were calculated from the difference in area (expressed in hectares) occupied by all cumulative disturbance objects existing between two consecutive years, and then standardized by total extent of the study area (expressed as $km^2$), leading to a summary statistic measured in $ha/km^2/yr$. Given that one $km^2$ equals 100 ha, this summary statistic for annual rate of change is equivalent to the percent area of change per year relative to the total study area. In order to summarize the spatial and temporal distribution of changes in disturbance features and in land-cover pattern, the study area was tesselated into equal-sized, non-overlapping square landscape cells (Figure 3). Each cell measured 49 $km^2$ (i.e., 7 km x 7 km), for a total of 178 landscape units. The cells coincided with a grid previously established for grizzly bear DNA hair-sampling in the study area (Boulanger *et al.* 2005, 2006) in order to enable the inferences of relationships that we will report in a subsequent study. The selected cell size achieved a balance between sample size, spatial detail (smaller extent yields more samples and higher spatial detail) and boundary effects (larger extent reduces the relative occurrence of artificially truncated landscape patches) (Leitão *et al.* 2006). Mean elevation and terrain ruggedness (the standard deviation of elevation) were computed from a 30 m digital elevation model (DEM) as supplemental information for each landscape cell. The DEM is a commercial model from the Canadian company DMTI Spatial, and acquired for this study through an academic agreement with the University of Calgary library. The model was created through interpolating the National Topographic Database 1:50,000 digital map contours, contours, spot heights, and water body polygons. A smoothing algorithm (Hutchinson, 1989) was used to eliminate 'stepping' and 'pit' artifacts commonly associated with similar medium-quality elevation models.

Disturbances were monitored by quantifying the density and proximity of all accumulated features between the years 1998 and 2005, based on the D-I vector layer (Table 1). The collection of disturbance objects existing in a particular year-of-interest was identified by selecting the year of origin (i.e., disturbance year) and then summarizing them both cumulatively, to represent total disturbance, as well as annually, to represent new disturbances. All cumulative estimates were derived by creating spatially explicit temporary maps using ArcGIS 9.3 (Esri 2008). These temporary maps were designed to avoid overestimating the total area of disturbance that could arise from overlapping disturbance features (e.g., a mine that was established over a previously harvested cutblock area).

* Table 1 here *

Specifically, *total cumulative disturbance density* was measured as the proportion of area occupied by all disturbance types for each landscape cell present by a given year, expressed in ha/km$^2$ (Table 1). In order to demonstrate the disturbance dynamics from year to year, the *density of annual disturbances* was calculated by summing all the disturbance objects originating in each respective year. Although these indicators were strictly structurally based, and assumed (conservatively) that the actual area impacted by any given disturbance type was the same across all disturbance types, they were chosen for their simplicity as a measure of overall disturbance magnitude. *Densities of the specific disturbance types* were computed cumulatively for the years

1998 and 2005, using standard indicators such as the areal proportion of cutblocks and surface mines (ha/km$^2$), density of wellsites (#/km$^2$) and linear density of roads and pipelines (km/km$^2$). For additional analytical insight, the size and number of cutblocks were also computed (Table 1). Natural fires were not reported as part of this list, since there was only one occurrence which occupied parts (340 ha) of one southern landscape cell in the year 2001. *Disturbance proximity* was represented as the mean nearest-neighbour distance to disturbance features within each landscape cell, measured both for all cumulative disturbances existing in a given year, and for all annual new disturbances arising between years (Table 1). The proximity calculations were performed through the generation of Euclidian-distance surfaces of 30m grain with Spatial Analyst within ArcGIS 9.3 (Esri 2008), wherein each grid cell stored the straight-line distance to the nearest disturbance feature. In order to quantify the association between relief and human disturbance, we computed Pearson correlation coefficients (r), measuring the strength of the linear relationship, between total cumulative disturbance density, elevation and terrain ruggedness.

For the summary of changes in land-cover pattern, this study focused on tracking four landscape-pattern metrics for each landscape cell over the seven-year monitoring horizon. As a simple measure of landscape composition, the area occupied by the dominant land-cover class in the region was selected and summarized as *percent forest area* (i.e., upland trees) based on its areal coverage of the landscape cell. In order to track changes in landscape structure caused by disturbance, three independent measures of landscape configuration were selected from six parsimonious metric groups based on group strength (i.e., explanatory power) (Linke and Franklin 2006, Cushman *et al.* 2008), including *mean patch size* (average size of all patches within the landscape cell), *largest patch index* (the percent area occupied by the largest contiguous patch within the landscape cell), and *mean shape index* (average compactness of patches). These three metrics quantitatively capture different aspects of the aggregate properties of the mosaic of land-cover patches when calculated at the landscape level. The metrics were calculated using *Fragstats* 3.3, software build 5 (McGarigal *et al.* 2002). For brevity of presentation, the four metrics were presented in a spatially implicit fashion, tracking their mean values across the 178 landscape cells over the eight years of the monitoring time frame. However, for visualization of land-cover pattern change, one landscape cell was selected as an example for graphical display of its land-cover map, alongside the tracking of its metric values over time (Figures 3 and 8). The mean values for all indicators of disturbance features and land-cover pattern were compared between 1998 and 2005, testing for significant differences using a significance level (α) of 0.05 in each of those metrics between the two years using one-tailed Welch's *t*-test, which allowed for unequal variances, using S-Plus statistical software (version 8.0, Insightful Corp. 2007).

## 4. Results

Over the seven-year monitoring horizon, the total area of change detected in the study area was 385 km$^2$, (i.e., 4.4 % of the study area), corresponding to a mean annual rate of change of 0.63 ha/km$^2$/yr (i.e., 0.63%/yr) (Figure 4). Annual rates of change remained relatively close to the mean, with a maximum fluctuation of 22% (i.e., maximum rate of 0.77 ha/km$^2$/yr) occurring between the years 2002 and 2003 (Figure 4).

* Figure 4 here *

### *4.1 Temporal and Spatial Distribution of Disturbance Features between 1998 and 2005*

Substantial change in disturbance density occurred over the seven-year time span, with the total cumulative disturbance density increasing by nearly 70%, from 6.3 to 10.7 ha/km$^2$ (Table 2). Increases in disturbance density occurred primarily along the central and eastern portions of the study area, across 79 % of all landscape cells (Figure 5B). A third of all cells exhibited mean rates of change above the overall average of 0.63% per year (i.e., 4.4 ha/km$^2$ increase between 1998 and 2005, Figure 5B), while over a fifth of all cells displayed mean rates above 1% per year (i.e., >7 ha/km$^2$ increase between 1998 and 2005, Figure 5B). Most of the disturbances occurred steadily over the years, with new, annual disturbances generally arising within the same or nearby landscape cells from year to year, and many exhibiting rapid rates of change: as high as 16 ha/km$^2$ (Figure 5C). The variation in cumulative disturbance density in 2005 was high across the 178 landscape cells, with about 20% of all cells containing disturbance densities between 20 and 42 ha/km$^2$, and leaving only 11% of all landscape cells completely undisturbed along the western boundary (Figure 5A).

* Table 2 and Figure 5 here *

The largest contributor to cumulative disturbance density and to the overall annual rate of change between 1998 and 2005 was of cutblock type. Their cumulative density alone accounted for 47% of all disturbances in 1998, and 64% in 2005 (Table 2). Over the seven years, the cumulative density of cutblocks more than doubled (~130% increase) across the study area, exhibiting a significant increase in mean density from 3 to 6.9 ha/km$^2$ (Table 2), equating to an annual rate of change of 0.55 ha/km$^2$. With an average size of 20.9 ha (standard error of 0.43), the cumulative number of discrete features of this disturbance type increased by the same proportion as its area-based density estimate (i.e.,130%), growing from a total of 901 cutblocks in 1998, to 2055 in 2005. This represented a number-based annual rate of change of about 1.9

cutblocks/100km$^2$. Cutblocks greatly expanded their occurrence from 58 to 85% of all landscape cells over that same time frame (Figure 6A). Across these cells, cumulative cutblock density varied greatly, ranging up to 42 ha/km$^2$ in 2005, with a similarly large range of density increases observed between the seven years (Figure 6A). Surface mines occurred in only two localized regions, and extended in total over less than 7% of all landscape cells (Figure 6B). Mines occupied an absolute area of 3621 ha in 1998 and 4790 ha in 2005, an increase of 32%. Mines accounted for only a small overall portion of the annual rate of change, with a total increase of 0.13 ha/km$^2$ over the entire study area (Table 2) and an average annual rate of change of about 0.02%. However, individual landscape cells contained substantial cumulative mine densities up to 18 ha/km$^2$ (Figure 6B).

* Figure 6 here *

Between 1998 and 2005, the average number of wellsites increased significantly by 7.1 wells per 100 km$^2$ from a cumulative density of about 10.7 to 17.8/100km$^2$. This represents a mean annual rate of change of about 1 site per 100km$^2$, and a 67% increase in cumulative density between 1998 and 2005 (Table 2). The overall occurrence of wellsites expanded slightly (i.e., well presence increased from 70 to 76% of all landscape cells, between 1998 and 2005), but most of the density increases were attributed to additional wells in cells already containing some level of this disturbance type. This was particularly true of cells situated along the midline and eastern boundary of the study area (Figure 6C). While wellsites reached a cumulative density above 100 wells/100km$^2$ in three landscape cells by 2005, the majority of cells containing this disturbance type remained at densities below 50 wells/100km$^2$ (Figure 6C). However, density increases were above the overall rate of change for over half of all landscape cells containing wells (i.e., 59 of 109 cells with density increases >7/100km$^2$ between 1998 and 2005, Figure 6C), and six cells exhibited density increases as high as five-times the overall rate of increase (increases >35/100km$^2$ between 1998 and 2005, Figure 6C). Linear-disturbance features, such as roads and pipelines, already existed throughout the majority of the study area (>87% of all landscape cells) at the beginning of the monitoring horizon (Figure 6D), but their cumulative overall density increased by a fourth from an average of 0.56 to 0.70 km/km$^2$ by 2005 (Table 2): a mean annual rate of change of 0.02km/km$^2$. Across individual landscape cells, cumulative densities varied considerately, ranging up to a maximum density of 2.6 km/km$^2$ by the year 2005. Net density increases varied considerately less for most landscape cells, with the majority of cells consistently gaining less than twice the mean annual rate of change (i.e., 0.26 km/km$^2$ between 1998 and 2005, Figure 6D).

Accompanying the significant increase in cumulative disturbance magnitude was a statistically insignificant (p-value 0.15), but nevertheless considerable (i.e.,20%) overall increase in disturbance proximity of almost 300m (Table 2). While proximities varied highly across space and time (Table 2, Figure 7A), the average distance between disturbance features decreased from about 1500 m in 1998 to 1200m in 2005. With the exception of a few landscape cells, every portion of the study area experienced decreases in mean distance to disturbance, ranging from a few meters to as much as 2000 m (Figure 7A, B). Furthermore, the number of landscape cells containing disturbances at an average distance of 200m or less increased substantially from three to 25 (Figure 7A) between 1998 and 2005. The proximity to new annual-disturbance features was much lower, with mean distances of around seven km across the seven years. Proximity to new annual features was consistently greater than five kilometers in the southwestern portion of the study area, and was highest along the eastern half of the study area, where landscape cells consistently exhibited mean distances of less than five km, but ranging as low as 410m (Figure 7C).

* Figure 7 here *

***4.2 Multi-temporal Change in Land-cover Pattern between 1998 and 2005***

Significant changes were observed for all four selected landscape pattern metrics, when comparing their mean values across all 178 landscape cells between 1998 and 2005 (Table 2, Figure 8). The area occupied by forest (i.e., upland trees) averaged 80% across landscape cells in 1998, and decreased steadily from year to year to an average of 75.7% in 2005 (Table 2, Figure 8-3A). Similarly steady annual decreases were exhibited for the mean values across measures of patch size, largest patch index, and mean shape index (Table 2, Figure 8-3B,C,D). Net relative decreases ranged from about 22% for mean patch size, 13% for largest patch size index, and about 2% for mean shape index (Table 2).

* Figure 8 here *

Within individual landscape cells, landscape metrics were observed to decrease substantially more erratically and to a higher overall degree than the averages reported above. For example, a landscape cell exposed to a large increase in cumulative disturbance density of 20.5 ha/km$^2$ between 1998 and 2005 exhibited a steep decrease in forest area from 88 to 67.5% (Figure 8-1, 2, 3A). Most of this change occurred between 1999 and 2003, and again between 2004 and 2005 (Figure 8-3A). The origins of these changes mainly constisted of new cutblocks, although new road segments were also constructed in 2000, 2002, and 2003, alongside new wellsites in 2000 and 2005 (Figure 8-1,2). Accompanying these disturbances, the average size of all patches existing in the landscape cell decreased by 53%, from 56ha in 1998 to 26ha in 2005 (Figure 8-3B). Patch shapes became more compact on average across the landscape, with a reduction in shape index from 2.0 to 1.7 (Figure 8-3D). While this example cell was already substantially dissected by disturbances in 1998, new roads and cutblocks further fragmented this cell, with the largest contiguous patch measuring only 17% in the time period following 2002 (Figure 8-3C).

## 5. Discussion and Conclusions

### *5.1 Disturbances and Change between 1998 and 2005*

The D-I framework to landscape monitoring generated a complete collection of spatially and temporally discrete disturbance features for the foothills study area, which enabled the estimation of landscape change between 1998 and 2005. Over this time frame, the region as a whole experienced a mean annual rate of change of 0.63%, leading to an increase in mean cumulative area covered by disturbances from 6.3 to 10.7 ha/km$^2$. As a means of comparison, the following mean annual rates of change were observed across a selection of other large-area monitoring studies in temperate forest ecosystems of North America:

- 0.25 % between 1973 and 2008 in the Kakwa, an area situated north to the Foothills study area (White *et al.* 2011);
- 0.49% in interior British Columbia between 1975 and 1992 (Sachs *et al.* 1998);
- 0.53% in the Klamath-Siskiyou ecoregion, Oregon and California between 1972 and 1992 (Staus *et al.* 2002);
- 1.19 % in the Oregon Cascades between 1972 and 1988 (Spies *et al.* 1994); and
- between 0.5 and 1.2 % in Western Oregon over successive intervals between 1972 and 1995 (Cohen *et al.* 2002).

The mean annual rate of change detected in the Foothills study area would therefore be considered *moderate* by comparison. Nevertheless, the tessellation of the Foothills area into 178, 7-km square cells enabled the detection of very rapid change throughout considerate portions of the landscape, especially in the eastern half, where there were 38 cells with an observed annual change rate of over 1%. Disturbance density increases did not appear to be limited by the occurrence of previously existing disturbances. On the contrary, new disturbances were spatially auto-correlated with existing disturbances, leading to high cumulative disturbance densities between 20 and 46 ha/km$^2$ in the central and eastern portions of the study area. Rugged terrain and high elevation were inversely correlated with disturbance density (Pearson correlation coefficient $r > 0.7$) across the cells, indicating that limited access along the western boundary constrained new disturbances in 21% of all cells, thereby adding more disturbance pressure on the more-accessible eastern and central portions of the study area.

The dominant change agent cited in studies outside of Alberta was timber harvesting, while both the Kakwa and foothills areas located within the province contained substantial additional disturbance types. In such multi-use landscapes, despite heavy apparent use, the overall annual rate of change may appear lower in comparison to other forest regions, for the sole reason that some disturbance types contribute relatively less area than timber cutblocks. This is due to both the relatively small size of oil and gas well sites, and the relatively low area-to-perimeter ratio of roads and pipelines. While the Kakwa study undertook important long-term monitoring of the temporary and spatial dynamics of change caused by all disturbance types combined (White *et al.* 2011), a disturbance-specific analysis, enabled through the use of a D-I framework such as the one undertaken in this study, constitutes an essential step forward providing comprehensive monitoring results in such multi-use landscapes.

Relative to the beginning of the monitoring horizon, cutblocks increased their cumulative density by 130%. With an annual rate of change of 0.55%, new cutblocks were the largest contributor (87%) to the overall annual rate of change of 0.63%, and thereby constituted the highest-growing disturbance type across the study area. Cutblocks passed from representing about half of all the area covered by disturbances at the beginning of the monitoring horizon, to representing nearly two-thirds by the year 2005. While surface mines expanded over the seven years, the disturbance was localized, and contributed just 3% of the overall annual rate of all change. The remaining 10% of the overall annual rate of change (i.e., 0.06%/yr) was accounted by roads/pipelines and well sites, which also have a very low contribution to area-based metrics. Notwithstanding, these disturbance types exhibited substantial and significant increases between 1998 and 2005 when their densities are represented by their length ($km/km^2$), in the case of roads/pipelines, and by their number ($\#/100km^2$), in the case of wellsites.

On a number-of-new-features basis, wellsites constitute the second fastest growing disturbance type in the Foothills, with an annual growth rate of 1 wellsite/$100km^2$: slightly above half the annual rate exhibited by forestry cutblocks (i.e., 1.9 discrete cutblocks/$100km^2$). The mean cumulative density of 17.8 wells/$100km^2$ in 2005 is well within the reported mean density for this area, as described by independent data for the entire province of Alberta for the year 2008 (Lee *et al.* 2009), and which places this study area in the below 1 well/$km^2$ category. Considering, however, that: (1) more than half of the landscape cells containing wellsites exhibited above-average annual rates, some of which were even above five-fold average rates; and (2) three landscape cells reached cumulative densities already above 1 well/$km^2$ in the year 2005; it can be speculated that the majority of this study area will move into the next provincial density category (1-2 wells/$km^2$) over the coming decade. Furthermore, the rate of cumulative wellsite development of 9.6% per year in the study area is higher than the average annual increase of 7.7% documented across the larger Boreal Plain ecoregion by Lee *et al.* (2009) between 1999 and 2008. Finally, new roads and pipeline sections were added in support of the two fastest-growing industries – forestry and oil and gas – at an overall annual rate of $0.02km/km^2$, with a fairly uniform overall distribution, to a cumulative density of 25% by 2005.

In summary, while the overall areal coverage by disturbances is moderate compared to other cited monitoring studies, the spatially explicit, disturbance-specific analysis demonstrated that a considerable portion of the study area is undergoing rapid change associated with a combination of forestry, oil and gas industry, and road/pipeline construction. As a result, this area has become increasingly accessible to humans, as measured by disturbance proximity. With a 300m decrease in the average distance to any disturbance feature over the seven-year monitoring horizon, the study area is rapidly becoming exposed to industrial development, leaving little room for wildlife to roam free and undisturbed. Moreover, in 25 out of the 178 foothills landscape cells (i.e.,14%), industrial development had reached a level in 2005 where any point within those cells was less than 200m away from a disturbance feature.

### *5.2 Land-cover Patterns between 1998 and 2005*

The trajectories of the selected metrics of land-cover pattern overall reflected the increasing loss of mature forest, and the fragmentation of the foothills landscape mosaic due to the growing levels of cumulative disturbance. The average percent forest area directly reflected the 4.4% total change, and decreased from 80% in 1998 to 75.7% by 2005. At the scale of individual landscape cells, forest loss was more conspicuous in cells of high change, where, for example, an overall 20.5% change (i.e., 20.5ha/km$^2$ cumulative density increase in disturbances between 1998 and 2005) reduced the percent forest area from 88 to 67.5 over the seven years.

The configuration of the foothills landscape exhibited consistent (i.e., for the average across the entire study area) and substantial (i.e., for individual landscape cells of high change) decreases in mean patch size, largest patch index and mean shape index, which have been well-documented as part of the *fragmentation syndrome*, wherein increasing forest losses are mirrored by associated changes in these metrics (Tinker *et al.* 1998; Staus *et al.* 2002). At such a landscape scale, roads and clearcuts have been associated with landscapes displaying: (1) more simplified, compact, less convoluted shapes (i.e., lower mean shape index); and (2) dissected large patches and perforated forest matrix reducing the overall mean size of patches (e.g., Reed *et al*. 1996a,b, Tinker *et al.* 1998, Hawbaker *et al.* 2006). When compared to other study regions exposed to much longer time frames of historic industrial development (e.g., Reed *et al.* 1996b, Hawbaker *et al.* 2006), the landscape heterogeneity and fragmentation of the foothills study area was relatively low in 1998, given the overall large expanse of forest cover. However, it is exactly in such landscapes where fragmentation impacts are relatively high (Linke *et al.* 2008). This could be observed in individual high-change landscape cells, where large decreases above 50% for mean patch size and 40% for largest patch index were observed over the fairly short time frame of seven years. This alone is a compelling reason to further monitor the Alberta foothills and similar multi-use forest areas, and to start investigating the possible systemic fragmentation impacts of the combined disturbances on the ecosystem. While the results of the land-cover pattern analysis presented here are sufficiently alarming, any further interpretations need to account for the fact that the area covered by disturbances in this study was computed conservatively, by only including the actual area covered as indicated by the satellite images. Frequently, buffers in the range up to 500m or more are added to estimate the effective disturbance area based on assumptions or wildlife probability distribution models (e.g., Leu *et al.* 2008, Lee *et al.* 2009), and would certainly have resulted in even higher disturbance and fragmentation rates.

***5.3 Framework Contribution and Future Research***

The D-I framework enabled the analysis of change by specific disturbance types, as well as the consistent representation of land-cover pattern over a multi-temporal time span. The boundary-conditioning rules of the framework are not only essential to the suppression of error propagation (Linke *et al.* 2009), they also enabled the accommodation of different data types and of manual vs. automated origin, as was the case in this study. The framework also forms an adaptable basis that is suitable for monitoring of different applications across landscapes, and can incorporate input from remote sensing data, and/or additional GIS data sources. Furthermore, with all disturbance objects represented as discrete entities over space and time, the D-I database provides a flexible and straightforward approach to landscape monitoring. Spatially explicit layers for each disturbance type and time step can be independently generated or transparently combined, depending on the application. Such layers could then be used as inputs for spatially explicit wildlife distribution models, or simply serve as a more detailed analysis of the structural characteristics of the human footprint (e.g., cutblock size, shape, frequency distribution etc).

The disturbance-specific analysis in this paper clearly documented the rapidly changing landscape in the study area, caused mainly by forestry and oil and gas exploitation, and the road/pipeline developments that accompany these industries. The rates of change and the associated landscape fragmentation call for ongoing monitoring of this and other similar multi-use landscapes. In future studies, we believe that important insight will be gained by studying the independent and cumulative effects of the specific disturbance types on landscape pattern change. The D-I database contains all the information necessary for spatially explicit modelling exercises designed to reveal the effects of different combinations of disturbance types. Last but not least, investigations into the systemic impacts of the combined disturbances on wildlife populations, based on outputs such as those presented in this paper, seem crucial for effective environmental management and conservation.

## 6. Acknowledgements

We thank Dr. Marie-Josée Fortin for her support and critical feedback to the first version of this manuscript. We are also grateful to Dr. Guillermo Castilla for constructive review comments throughout the research period of this manuscript. This work has been funded in part through the Natural Science and Engineering Research Council of Canada (NSERC) grant to Gregory J. McDermid. Julia Linke was directly supported by an Alberta Ingenuity Award for the data preparation phase of this research, and by a NSERC post-doctoral fellowship for the analysis and writing phase. We gratefully acknowledge the support of Foothills Research Institute Grizzly Bear Research Program and its many partners in government, academics, and industry.

## 7. References


Alberta Grizzly Bear Recovery Plan 2008-2013 (AGBRP). 2008. Alberta Sustainable Resource Development, Fish and Wildlife Division, Alberta Species at Risk Recovery Plan No. 15.Edmonton, AB. 68 pp.

Alberta Sustainable Resource Development and Alberta Conservation Association (ASRD/ACA) (2010a). Status of the Woodland Caribou (Rangifer tarandus caribou) in Alberta: Update 2010 (pp. 88), Edmonton, AB: Alberta Sustainable Development.

Alberta Sustainable Resource Development and Alberta Conservation Association (ASRD/ACA) (2010b). Status of the Grizzly Bear (Ursus acrtos) in Alberta: Update 2010 (pp. 44), Edmonton, AB: Alberta Sustainable Development.

Ahlqvist, O. (2008). Extending post-classification change detection using semantic similarity metrics to overcome class heterogeneity: A study of 1992 and 2001 U.S. National Land Cover Database changes, *Remote Sensing of Environment*, 112, 1226-1241

Balmford, A., Green, R.E., & M. Jenkins. (2003). Measuring the changing state of nature, *Trends in Ecology and Evoloution* 18(7), 326-330.

Beckingham, J. D., Corns, I.G.W., &Archibald, J.H. (1996). Field Guide to Ecosites of West-Central Alberta. Natural Resources Canada. Canadian Forest Service, Northwest region, Northern Forestry Centre, Edmonton, Alberta.

Blaschke, T. (2005). A framework for change detection based on image objects, *Göttinger Geographische Abhandlungen*, S. Erasmi, B. Cyffka, and M. Kappas, Eds., 113, 1–9.

Boulanger, J., Stenhouse, G., Proctor, M., Himmer, S., Paetkeau, and J. Cranston, 2005a. Population inventory and density estimates for the Alberta 3B and 4B Grizzly Bear Management Areas. Alberta Sustainable Resource Development. Edmonton. 31 pp.

Boulanger, J., M. Proctor, S. Himmer, G. Stenhouse, D. Paetkau, and J. Cranston, 2006. An empirical test of DNA mark–recapture sampling strategies for grizzly bears. *Ursus* 17:149–158.

Brown, D.G., Duh, J.-D., & Drzyzga, S.A. (2000). Estimating error in an analysis of forest fragmentation change using North American Landscape Characterization (NALC) data, *Remote Sensing of Environment*, 71,106-117.

Carmel, Y., Dean, D.J., & Flather, C.H. (2001). Combining location and classification error sources for estimating multi-temporal database accuracy, *Photogrammetric Engineering and Remote Sensing* 67,865-872.

Chrisman, N.R. (1989). Modelling error in overlaid categorical maps (pp. 21-34). In M.F. Goodchild & S. Goopal (Eds.). Accuracy of spatial databases. London, U.K.: CRC Press

Cohen, W.B., Spies, T.A., Alig, R.J., Oetter, D. R., Maiersperger, T.K., & Fiorella, M. (2002). Characterizing 23 Years (1972–95) of Stand Replacement Disturbance in Western Oregon Forests with Landsat Imagery, *Ecosystems* 5, 122-137.

Coppin P., Jonckheere, I., Nackaerts, N., Muys, B., & Lambien, E. (2004). Digital change detection methods in ecosystem monitoring: a review, *International Journal of Remote Sensing*, 25(9),1565-1596

Cushman, S.A., & McGarigal, K. (2006). Multi-variate landscape trajectory analysis: An example using simulation modeling of American marten habitat change under three disturbance regimes (pp. 119-140). In J.A. Bissonette & I. Storch (Eds.) Temporal Explicitness in Landscape Ecology: Wildlife Responses to Changes in Time. New York: Springer-Verlag

Cushman, S.A., McGarigal, K., & Neel, M. (2008). Parsimony in landscape metrics: strength, universality, and consistency, *Ecological Indicators*, 8,691-703.

Desclée, B., Bogaert, P., & Defourny, P. (2006). Forest change detection by statistical object-based method, *Remote Sensing of Environment*, 102, 1-11.

Esri, 2008. ArcMap 9.3: ArcGIS Desktop 9.3 Service Pack 1 (Build 1850), Redlands, CA.

Feranec, J., Hazeu, G., Christensen, S., & Jaffrain, G. (2007). Corine land-cover change detection in Europe (case studies of the Netherlands and Slovakia), *Land Use Policy* 24,234-247.

Franklin, S.E., Lavigne, M.B., Moskal, L.M., & McCaffrey, T.M. (2001). Interpretation of forest harvest conditions in New Brunswick using Landsat TM enhanced wetness difference imagery (EWDI), *Canadian Journal of Remote Sensing* 27,118-128.

Fry, J., Xian, G., Jin, S., Dewitz, J., Homer, C., Yang, L., Barnes, C., Herold, N., &Wickham, J. (2011). Completion of the 2006 National Land Cover Database for the Conterminous United States, *Photogrammetric Engineering and Remote Sensing*, 77(9),858-864.

Foley J. A., Defries, R., Asner, G. P., Barford, C., Bonan, G., Carpenter, S. R., Chapin, F. S., Coe, M. T., Daily, G. C., Gibbs, H. K., Helkowski, J. H., Holloway, T., Howard, E. A., Kucharik, C. J., Monfreda, C., Patz, J. A., Prentice, I. C., Ramankutty, N., & Snyder, P. K. (2005). Global consequences of land use, *Science*, 309(5734), 570-574.

Gergel, S.E. (2006). New Directions in Landscape Pattern Analysis and Linkages with Remote Sensing (pp. 173-208). In M.A. Wulder & S.E. Franklin (Eds.) Understanding Forest Disturbance and Spatial Pattern. Baton Rouge, LA: CRC, Taylor and Francis Group

Gillanders, S.N., Coops, N.C., Wulder, M.A., Gergel, S.E., & Nelson, T. (2008). Multi-temporal remote sensing of landscape dynamics and pattern change: describing natural and anthropogenic trends, *Progress in Physical Geography*, 32(2), 503-528.

Goodchild, M.F., (1978). Statistical aspects of the polygon overlay problem, *Harvard Papers on Geographic Information Systems*, 6.

Hansen, A.J., Neilson, R.P., Dale, V.H., Flather, C.H., Iverson, L.R., Currie, D.J., Shafer, S., Cook, R. & Bartlein, P.J. (2001). Global change in forests: responses of species, communities, and biomes, *Bioscience* 51, 765-779.

Hawbaker, T.J., Radeloff, V.C., Clayton, M.K., Hammer, R.B., & Gonzalez-Abraham, C.E. (2006). Road development, housing growth, and landscape fragmentation in Northern Wisconsin: 1937-1999, *Ecological Applications* 16(3),1222-1237.

Hess, G. (1994). Pattern and error in landscape ecology: A commentary, *Landscape Ecology*, 9, 3–5.

Houghton R.A., (1994). The worldwide extent of land-use change, *Bioscience* 44, 305-313.

Hutchinson, M. F., (1989). A new method for gridding elevation and stream line data with automatic removal of pits. *Journal of Hydrology*,106, 211-232.

Kerr, J.T., & Ostrovsky, M. (2003). From space to species: ecological applications for remote sensing, *Trends in Ecology and Evolution* 18, 299-305.

Lambin, E. F., Turner, B. L., Geist, H. J., Agbola, S. B., Angelsen, A., Bruce, J. W., Coomes, O. T., Dirzo, R., Fischer, G., Folke, C., George, P. S., Homewood, K., Imbernon, J., Leemans, 637 R., Li, X., Moran, E. F., Mortimore, M., Ramakrisnan, P. S., Richards, J. F., Sanes, H., Steffen, W., Stone, G. D., Svedin, U., Veldkamp, T. A., Vogel, C.,& Xu, J. (2001). The causes of land-use and land-cover change: moving beyond the myths, *Global Environmental Change*,11(4), 261-269

Langford, W.T., Gergel, S.E., Dietterich, T.G., & Cohen, W. (2006). Map misclassification can cause large errors in landscape pattern indices: examples from habitat fragmentation, *Ecosystems*, 9,474-488.

Lee, P.G., Hanneman, M., Gysbers, J.D., & Cheng, R. 2009. The last great intact forests of Canada: Atlas of Alberta. (Part II: What are the threats to Alberta's forest landscapes?) Edmonton Alberta: Global Forest Watch Canada. 145 pp. Available online: http://www.globalforestwatch.ca/WBWL/atlasofalberta/downloads.htm [accessed March 19, 2012].

Leitão, A.B., Miller, J., SAhern, J. & McGarigal K. (2006). Measuring landscapes: a planner's handbook (pp. 245). Washington, DC: Island Press

Leu, M., Hanser, S.E., & Knick, S.T. (2008). The human footprint in the west: a large-scale analysis of anthropogenic impacts, *Ecological Applications* 18(5), 1119-1139.

Li, H., & Wu, J. (2007). Landscape pattern analysis: key issues and challenges (pp.39-61). In J. Wu & R. Hobbs (Eds.) Key Topics in Landscape Ecology. Cambridge, U.K.: Cambridge University Press

Linke, J., Franklin, S.E., Huettmann, F., & Stenhouse, G.B. (2005). Seismic cutlines, changing landscape metrics and grizzly bear landscape use in Alberta, *Landscape Ecology* 20,811-826.

Linke, J. & Franklin, S.E. (2006). Interpretation of landscape structure gradients based on satellite image classification of land cover, *Canadian Journal of Remote Sensing* 32(6),367-379.

Linke, J., Franklin, S.E., Hall-Beyer, M., & Stenhouse, G.B. (2008). Effects of cutline density and land-cover heterogeneity on landscape metrics in western Alberta, *Canadian Journal of Remote Sensing* 34(4),390-404.

Linke, J., McDermid, G.J., Pape, A., McLane A.J., Laskin, D.N., Hall-Beyer, M. & Franklin, S.E. (2009a). The influence of patch-delineation mismatches on multi-temporal landscape pattern analysis, *Landscape Ecology* 24(2),157-170.

Linke, J., McDermid, G.J., Laskin, D.N., McLane A.J., Pape, A., Cranston, J., Hall-Beyer, M. & Franklin, S.E. (2009b). A disturbance-inventory framework for flexible and reliable landscape monitoring, *Photogrammetric Engineering and Remote Sensing* 75(8),981-995.

Linke, J., & McDermid, G.J. (2011). A conceptual model for multi-temporal landscape monitoring in an object-based environment, *IEEE – Journal of Selected Topics in Applied Earth Observations and Remote Sensing* 4(2),265-271.

Lu, .D., Mausel, P., Brondizio, E., & Moran, E. (2004). Change detection techniques, *International Journal of Remote Sensing* 25,2365-2407.

Loveland, T.R., Sohl, T.L., Stehman, S.V., Gallant, A.L., Sayler, K.L.& Napton, D.E. (2002). A Strategy for Estimating the Rates of Recent United States Land Cover Changes, *Photogrammetric Engineering and Remote Sensing* 68(10),1091-1099.

Mas, J.F. (2005). Change estimates by map comparison: a method to reduce erroneous changes due to positional error, *Transactions in GIS*, 9,619-629.

McDermid, G. J., Linke, J., Pape, A.D., Laskin D.N., McLane, A.J. & Franklin, S.E. (2008). Object-based approaches to change detection and thematic map update: challenges and limitations, *Canadian Journal of Remote Sensing* 34(5), 462-466.

McDermid, G.J. (2005). Ph.D. Thesis: Remote Sensing for Large-Area, Multi- Jurisdictional Habitat Mapping (pp.258), Waterloo, ON: University of Waterloo

McGarigal, K., Cushman, S.E., Neel, M.C., & Ene, E. (2002). FRAGSTATS: Spatial Pattern Analysis Program for Categorical Maps. Computer software program produced by the authors at the University of Massachusetts, Amherst. Available at the following web site: www.umass.edu/landeco/research/fragstats/fragstats.html

Newton, A.C., Hill, R.A., Echeverría, C., Golicher, D., Rey-Benayas, J.M., Cayuela, L., & Hinsley, S.A. (2009). Remote sensing and the future of landscape ecology, *Progress in Physical Geography* 33(4), 528-546.

O'Neill, R.V., Krummel, J.R., Gardner, R.H., Sugihara, G., Jackson, B., DeAngelis, D.L., Milne, B.T., Turner, M.G., Zygmunt, B., Christensen, S.W., Dale, V.H., & Graham, R.L. (1988). Indices of Landscape Pattern, *Landscape Ecology* 1,153-162.

Reed, R. A., J. Johnson-Barnard, & Baker, W.L. (1996a). Fragmentation of a forested Rocky Mountain landscape, 1950-1993, *Biological Conservation* 75, 267-277.

Reed, R. A., J. Johnson-Barnard, & Baker, W.L. (1996b). Contribution of roads to forest fragmentation in the Rocky Mountains, *Conservation Biology* 10,1098-1106.

Sachs, D.L., Sollins P. & Cohen, W.B. (1998). Detecting landscape changes in the interior of British Columbia from 1975 to 1992 using satellite imagery, *Canadian Journal of Forest Research* 28, 23-36.

Schneider, R. R., Stelfox, J. B. , Boutin, S. & S. Wasel. (2003). Managing the cumulative impacts of land uses in the Western Canadian Sedimentary Basin: a modeling approach. *Conservation Ecology* **7**(1), 8. [online] URL: http://www.consecol.org/vol7/iss1/art8/

Shao, G., Liu, D., & Zhao, G. (2001). Relationships of image classification accuracy and variation of landscape statistics, *Canadian Journal of Remote Sensing* 27,33-43.

Shao, G. & Wu, J. (2008). On the accuracy of landscape pattern analysis using remote sensing data, *Landscape Ecology* 23,505–511.

Singh,A. (1989). Digital change detection techniques using remotely-sensed data, *International Journal of Remote Sensing*, 10(6),989-1003.

Skole, D., Justice, C., Townshend, J. & Janetos, A. (1997). A land cover change monitoring program: Strategy for an international effort, *Mitigation and Adaptation Strategies for Global Change* 2(2),157-175.

Sohl, T.L., Gallant A.L. & Loveland, T.R. (2004). The characteristics and interpretability of land surface change and implications for project design, *Photogrammetric Engineering and Remote Sensing* 70(4),439-448.

Southworth, J., Nagendra, H. & Tucker, C. (2002). Fragmentation of a Landscape: incorporating landscape metrics into satellite analyses of land-cover change, *Landscape Research* 27(3),253-269.

Spies, T.A., Ripple, W.J., & Bradshaw, G.A. (1994). Dynamics and patterns of a managed coniferous forest landscape in Oregon, *Ecological Applications* 4, 555-568.

Staus, N.L., Strittholt, J.R., DellaSala, D.A., & Robinson, R. (2002). Rate and pattern of forest disturbance in the Klamath-Siskiyou ecoregion, USA between 1972 and 1992, *Landscape Ecology* 17, 455-470.

Strong, W.L. (1992). Ecoregions and ecodistrics of Alberta. Alberta Forests, Lands, Wildlilfe, Edmonton, Alberta, Publication T/244.

Sundaresan, A., Varshney, P.K. & Arora, M.K. (2007). Robustness of change detection algorithms in the presence of registration errors, *Photogrammetric Engineering and Remote Sensing* 73(4),375-383.

Tinker, D.B., Resoir, C.A.C., Beauvois, G.P., Kipfmueller, K.F., Fernandes, C.I., & Baker, W.L. (1998) Watershed analysis of forest fragmentation by clearcuts and roads in a Wyoming forest, *Landscape Ecology*, 13,149–165.

Turner, W., Spector, S., Gardiner, N., Fladeland, M., Sterling, E., & Steininger, M. (2003). Remote sensing for biodiversity science and conservation, *Trends in Ecology and Evolution* 18(6),306-314.

Vogelman, J. E.,Howard, S.M.,Yang,L.,Larson,C.R.,Wylie,B. K.,& VanDriel, N. (2001). Completion of the 1990 s national land cover data set for the conterminous United States for Landsat Thematic Mapper data and ancillary data sources, *Photogrammetric Engineering and Remote Sensing*, 67(6),650−655.

Walter, V. (2004). Object-based classification of remote sensing data for change detection, *ISPRS Journal of Photogrammetry and Remote Sensing* 58(3-4),225-238.

White, J.C., Wulder, M.A., Gómez, C., & Stenhouse, G. (2011). A history of habitat dynamics: Characterizing 35 years of stand replacing disturbance. *Canadian Journal of Remote Sensing* 37(2), 234-251.

Wickham, J.D., O'Neill, R.V., Riitters, K.H., Wade, T.G., & Jones, K.B. (1997). Sensitivity of selected landscape pattern metrics to land-cover misclassification in land-cover composition, *Photogrammetric Engineering and Remote Sensing* 63(4),397-402.

Woodcock, C.E., Allen, A.A., Anderson, M., Belward, A.S., Bindschadler, R., Cohen, W.B., Gao, F., Goward, S.N., Helder, D., Helmer, E., Nemani, R., Oreapoulos,L., Schott, J., Thenkabail, P.S., Vermote, E.F., Vogelman, J., Wulder, M.A., & Wynne, R. (2008). Free access to Landsat imagery, *Science* 320,1011.

Yuan, D., & Elvidge, C. (1998). NALC land-cover change detection pilot study: Washington D.C. area experiments, *Remote Sensing of Environment*, 66,166-178.

Xian, G., Homer, C., & Fry, J. (2009). Updating the 2001 National Land Cover Database land cover classification to 2006 by using Landsat imagery change detection methods, *Remote Sensing of Environment*, 113(6), 1133-1147.

**List of Figures**

**Figure 1**. The disturbance-inventory framework updates and backdates an object-based land-cover map at time $T_0$, which constitutes the reference for the monitoring horizon ($T_{-n}$ to $T_{+n}$). Changes are depicted with the use of dynamic objects (DO), that are detected as discrete entities of change, stored in a GIS-vector layer (i.e., disturbance inventory), and classified with their disturbance type, time of origin (i.e., disturbance year), and temporally relevant land-cover values for each time step ($LC_n$). These land-cover values are used to generate backdate and update layers for each time step, and then used to replace the spatially coinciding entities in new versions of the reference map representing spatially consistent depictions of landcover through time. The framework handles all the basic landscape dynamics, including feature *appearance* (e.g., feature C at $T_{-1}$), *disappearance* (e.g., feature B at $T_{+2}$), *persistence* (e.g., feature A between $T_0$ and $T_{+1}$), *succession* (e.g., feature A from $T_{-1}$ to $T_0$), *expansion* (e.g., feature D at $T_{+2}$), and *shrinkage* (e.g., feature B between $T_{-1}$, $T_0$ and $T_{+1}$) over time. Please note two exceptions: (1) while generally all DOs are unique, discrete entities, an object may be split if it straddles other objects in either the disturbance inventory or reference map, such as the case for feature C, and (2) a DO with time of origin *after* $T_0$, requires no value for $LC_{-n}$.

**Figure 2**. Spurious change artifacts in the backdated and updated maps can arise from unconditioned backdated and update layers, and are caused by mismatches between the boundaries of dynamic objects and those of the objects in the original reference map (i.e., *intersect objects*). Boundary undershoots can result in the introduction of *slivers* when mismatches occur between spatially coinciding features (*b* and *c* in backdated map $T_{-1}$, and *d* in updated map $T_{+1}$), and spurious *gaps* (e), when mismatches occur between adjacent features. However, if the land-cover attributes of the intersect objects and the coinciding reference map are the same, the artifacts will not appear (i.e., *d* in backdated map $T_{-1}$ and *b* and *c* in updated map $T_{+1}$). Present, but less apparent are boundary overshoots that result in objects spuriously appearing to be *stretched* in size (*a*) or to *encroach* an adjacent feature (*f*) when compared to the reference map.

**Figure 3**. Extent, context, and stratification of the 8721-km$^2$ Foothills study area into 49 km$^2$ landscape cells located in western-central Alberta, Canada in respect with Landsat Thematic Mapper imagery (path 45/row23) displayed in false-colour composite) . The insets depict an example landscape cell (outlined in red) showing the cumulative disturbance-inventory vector database (top; absent are two types: mine and fire) for the monitoring horizon (1998 to 2005), and the updated land-cover map (bottom; absent are four classes: water, snow/ice, shadow and cloud) at year 2005.

**Figure 4**. Year-to-year and mean annual rate of overall vegetation-replacing land-cover change observed in the 8721-km2 Foothills landscape over the monitoring time frame.

**Figure 5**. Distribution of (A) the disturbance density of all features accumulated by the years 1998 and 2005 (with inserts illustrating the disturbance density of the central landscape cell in addition to the graphical depiction of the actual cumulative disturbances present in each year), (B) the increase in disturbance density between 1998 and 2005, and (C) the disturbance density of any new features occurring in a specific year between 1998 and 2005.

**Figure 6**. Distribution of cumulative densities across landscape cells for the specific disturbance types, such as A) cutblocks, B) surface mine, C) wellsites, and D) roads and pipelines in the years 1998 and 2005, and their net density changes over these 7 years.

**Figure 7**. Proximity to (A) any nearest cumulative disturbance feature in 1998 and 2005 (with inserts illustrating mean proximity in the central landscape cell in addition to the graphical depiction of the actual distance surface of the given year), (B) associated decrease in nearest neighbour distance between 1998 and 2005, and (C) proximity to any nearest new feature arisen each year between 1998 and 2005.

**Figure 8**.  Spatially consistent land-cover map series in correspondence with Landsat Thematic Mapper imagery (displayed in false colour composite with bands 4, 3, 2 in channels red, green, blue) in a 7×7 km example landscape cell exposed to a high level of disturbance (same example cell, outlined in red colour, as displayed in Figure 1; cumulative disturbance density increased from 7 to 27.5ha/km2) between 1998 and 2005 and select indicators of landscape pattern, such as A) percent forest area, B) landscape-level mean patch size, C) largest patch index and D) mean shape index, calculated for the example cell shown and for the mean across all 178 cells.

## List of Tables

**Table 1**. Metrics used to monitor disturbance features and land-cover pattern across the sampled landscape cells of the study area over time (land-cover pattern metrics are computed according to McGarigal *et al.* 2002).

| Selected Metrics for Monitoring Analysis | Definition | Units |
|---|---|---|
| ***Disturbance Features*** | | |
| Total cumulative disturbance density | Total area covered by all disturbances that accumulated by a given year (i.e.,1998 or 2005) | (ha/km$^2$) |
| Annual disturbance density | Total area covered by of all new disturbances arisen in any single year between 1998 and 2005 | (ha/km$^2$) |
| Density of all cumulative cutblocks | Total area covered by all cutblocks that accumulated by a given year (i.e., 1998 or 2005) | (ha/km$^2$) |
| Density of all cumulative surface mines | Total area covered by all surface mines that accumulated by a given year (i.e., 1998 or 2005) | (ha/km$^2$) |
| Density of all cumulative wellsites | Total number of all wellsites that accumulated by a given year (i.e., 1998 or 2005) | (#/100km$^2$) |
| Density of cumulative linear features | Total length of roads and pipelines that accumulated by a given year (i.e., 1998 or 2005) | (km/km$^2$) |
| Mean proximity to nearest disturbance feature | Mean distance to any nearest disturbance feature accumulated by a given year (i.e., 1998 or 2005) | (m) |
| Mean proximity to nearest new, annual disturbance feature | Mean distance to any nearest new disturbance feature arisen in any year between 1998 and 2005 | (m) |
| ***Land-cover Pattern*** | | |
| Percent forest area | Total area occupied by forest expressed as a proportion of the area of the landscape cell | (%) |
| Mean patch size | Mean size of all discrete land-cover patches within a landscape cell | (ha) |
| Largest patch index | Largest contiguous land-cover patch within a landscape cell expressed as a proportion of area of the landscape cell | (%) |
| Mean shape index | Measures the average shape complexity of all land-cover patches based on perimeter-area relationships compared to a standard compact shape; the index is minimum at most compact average shape and increases as patches become more complexly shaped. | unitless |

**Table 2**. Comparison of the means for selected indicators for disturbance features and land-cover pattern between 1998 and 2005 across the study area (n=178 landscape cells; please note that probabilities are computed for one-tailed comparisons of the means using Welch's t-test and significant differences are indicated with * for α = 0.05)

| **Indicators** | **1998** | | **2005** | | **Probability** |
|---|---|---|---|---|---|
| | **Mean** | **SE** | **Mean** | **SE** | **P(μ1998-μ2005 > or < 0)** |
| ***Disturbance Features*** | | | | | |
| Total cumulative disturbance density ($ha/km^2$) | 6.30* | 0.45 | 10.7* | 0.73 | <0.000 |
| Density of all cumulative cutblocks ($ha/km^2$) | 2.99* | 0.33 | 6.85* | 0.59 | <0.000 |
| Density of all cumulative surface mines ($ha/km^2$) | 0.42 | 0.16 | 0.55 | 0.19 | 0.320 |
| Density of all cumulative wellsites ($\#/100km^2$) | 10.66* | 1.47 | 17.79* | 1.94 | 0.004 |
| Density of cumulative linear features ($km/km^2$) | 0.56* | 0.03 | 0.70* | 0.04 | 0.004 |
| Mean proximity to nearest disturbance feature (m) | 1474 | 139.9 | 1200 | 127.1 | 0.150 |
| ***Land-cover Pattern*** | | | | | |
| Percent area occupied by forest (%) | 80.02* | 1.15 | 75.67* | 1.19 | 0.004 |
| Mean patch size (ha) | 65.81* | 4.01 | 51.50* | 2.77 | 0.002 |
| Largest patch index | 53.65* | 1.77 | 46. 65* | 1.80 | 0.003 |
| Mean shape index | 1.80* | 0.01 | 1.76* | 0.01 | 0.004 |

Figure 1

Click here to download high resolution image

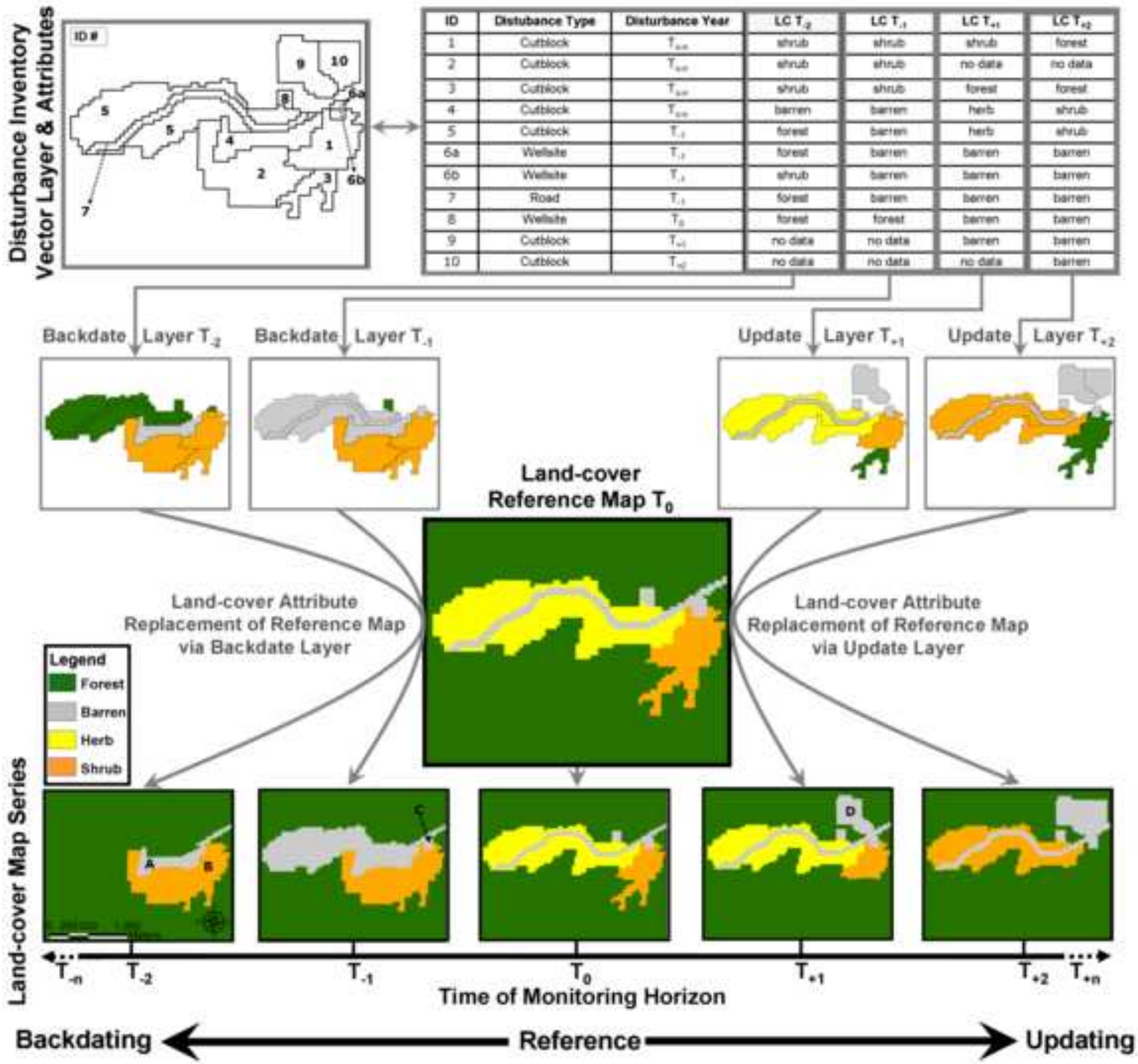


| ID | Distubance Type | Disturbance Year | LC $T_{-2}$ | LC $T_{-1}$ | LC $T_{+1}$ | LC $T_{+2}$ |
|---|---|---|---|---|---|---|
| 1 | Cutblock | $T_{-n}$ | shrub | shrub | shrub | forest |
| 2 | Cutblock | $T_{-n}$ | shrub | shrub | no data | no data |
| 3 | Cutblock | $T_{-n}$ | shrub | shrub | forest | forest |
| 4 | Cutblock | $T_{-n}$ | barren | barren | herb | shrub |
| 5 | Cutblock | $T_{-1}$ | forest | barren | herb | shrub |
| 6a | Wellsite | $T_{-1}$ | forest | barren | barren | barren |
| 6b | Wellsite | $T_{-1}$ | shrub | barren | barren | barren |
| 7 | Road | $T_{-1}$ | forest | barren | barren | barren |
| 8 | Wellsite | $T_0$ | forest | forest | barren | barren |
| 9 | Cutblock | $T_{+1}$ | no data | no data | barren | barren |
| 10 | Cutblock | $T_{+2}$ | no data | no data | no data | barren |

Figure 2
Click here to download high resolution image

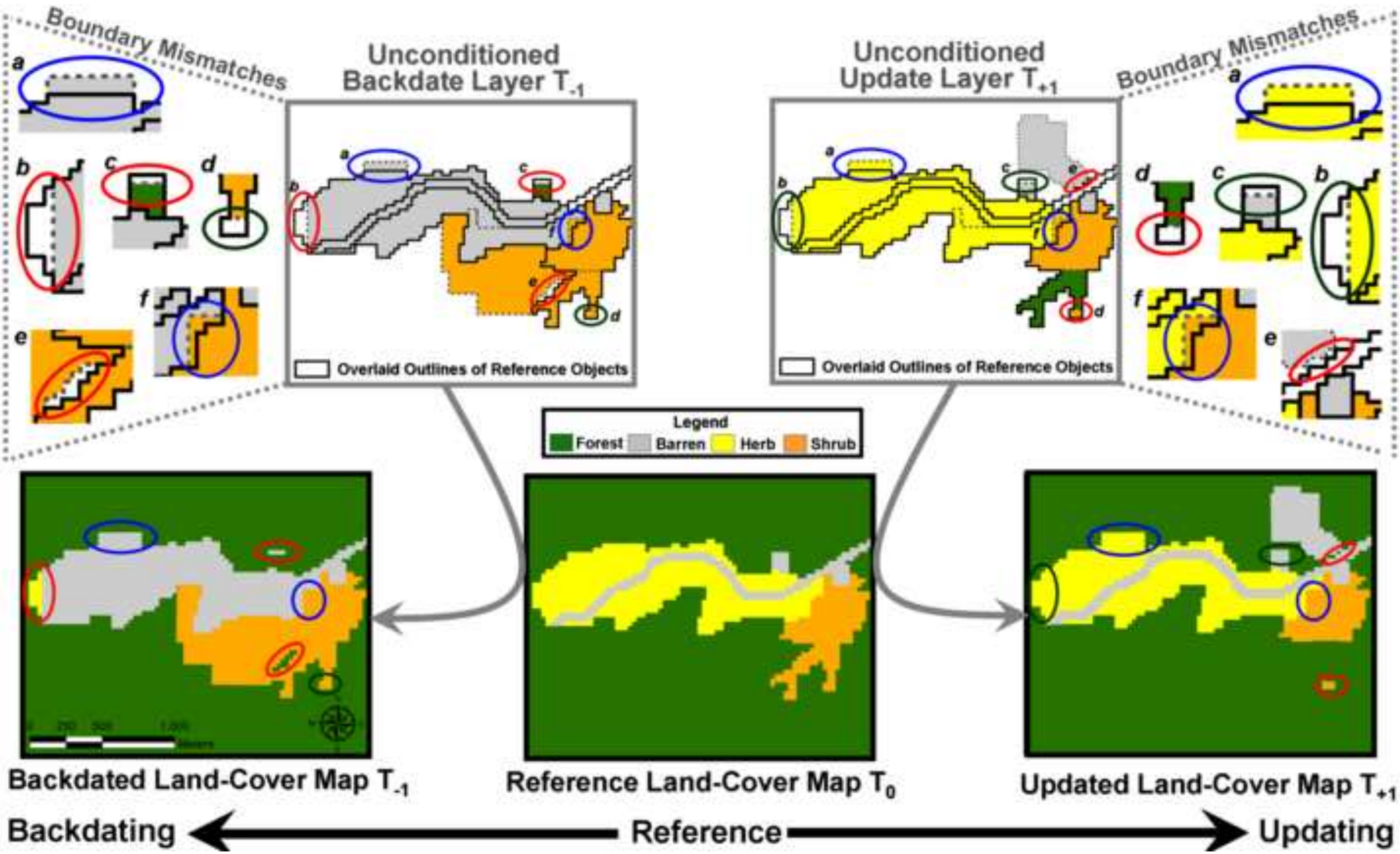

Figure 3
Click here to download high resolution image

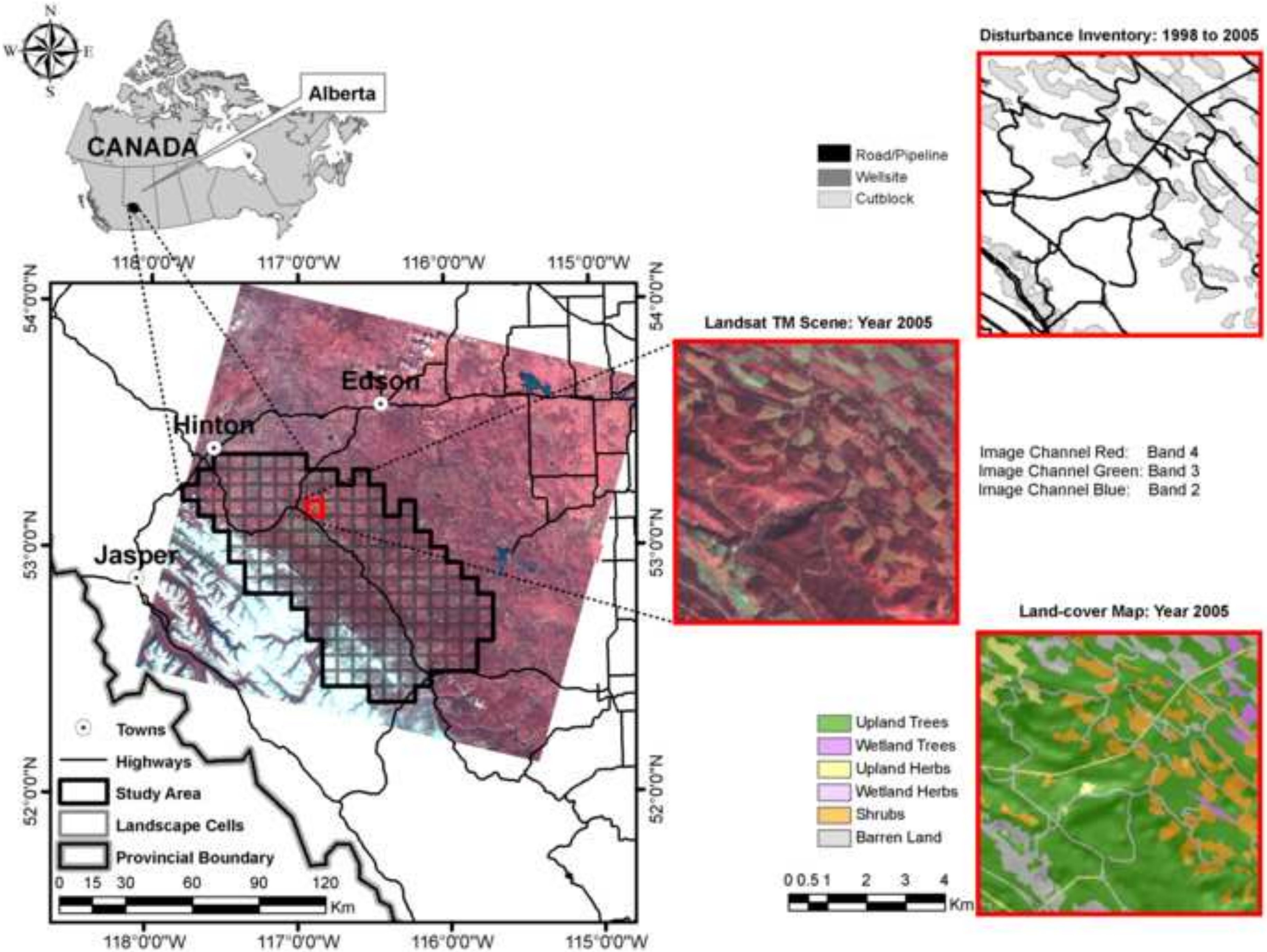

Figure 4
Click here to download high resolution image

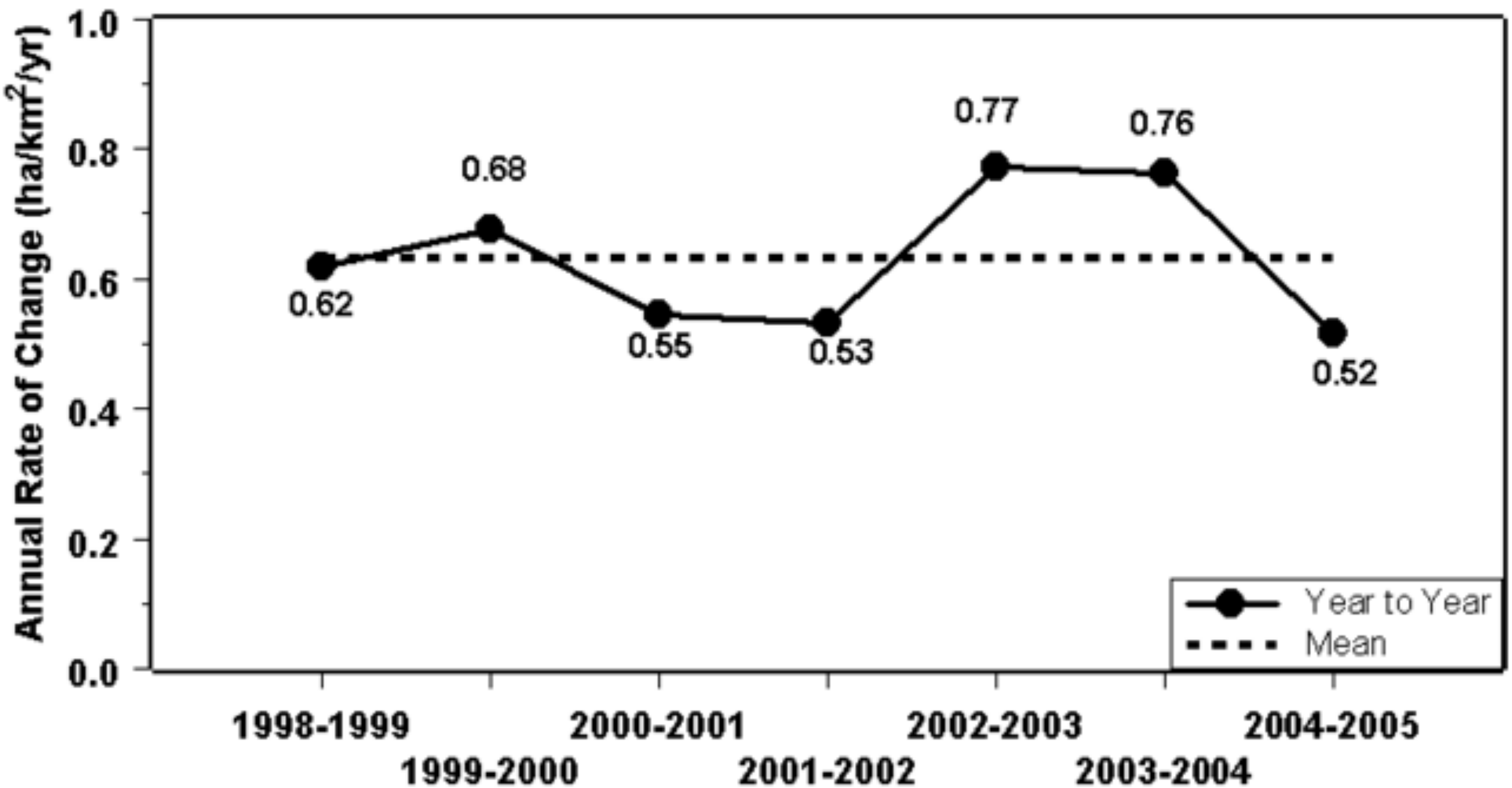

Figure 5

Click here to download high resolution image

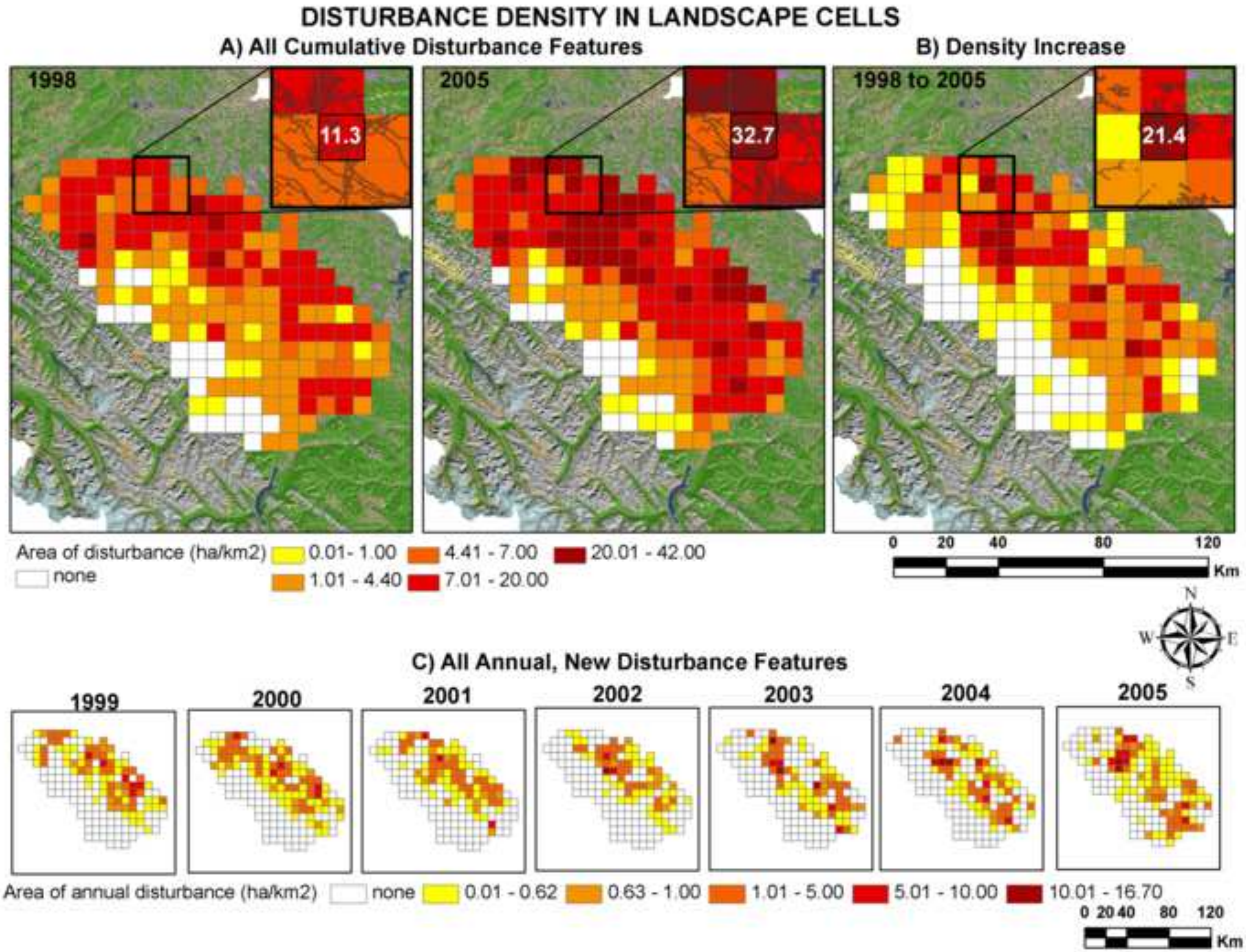

Figure 6

Click here to download high resolution image

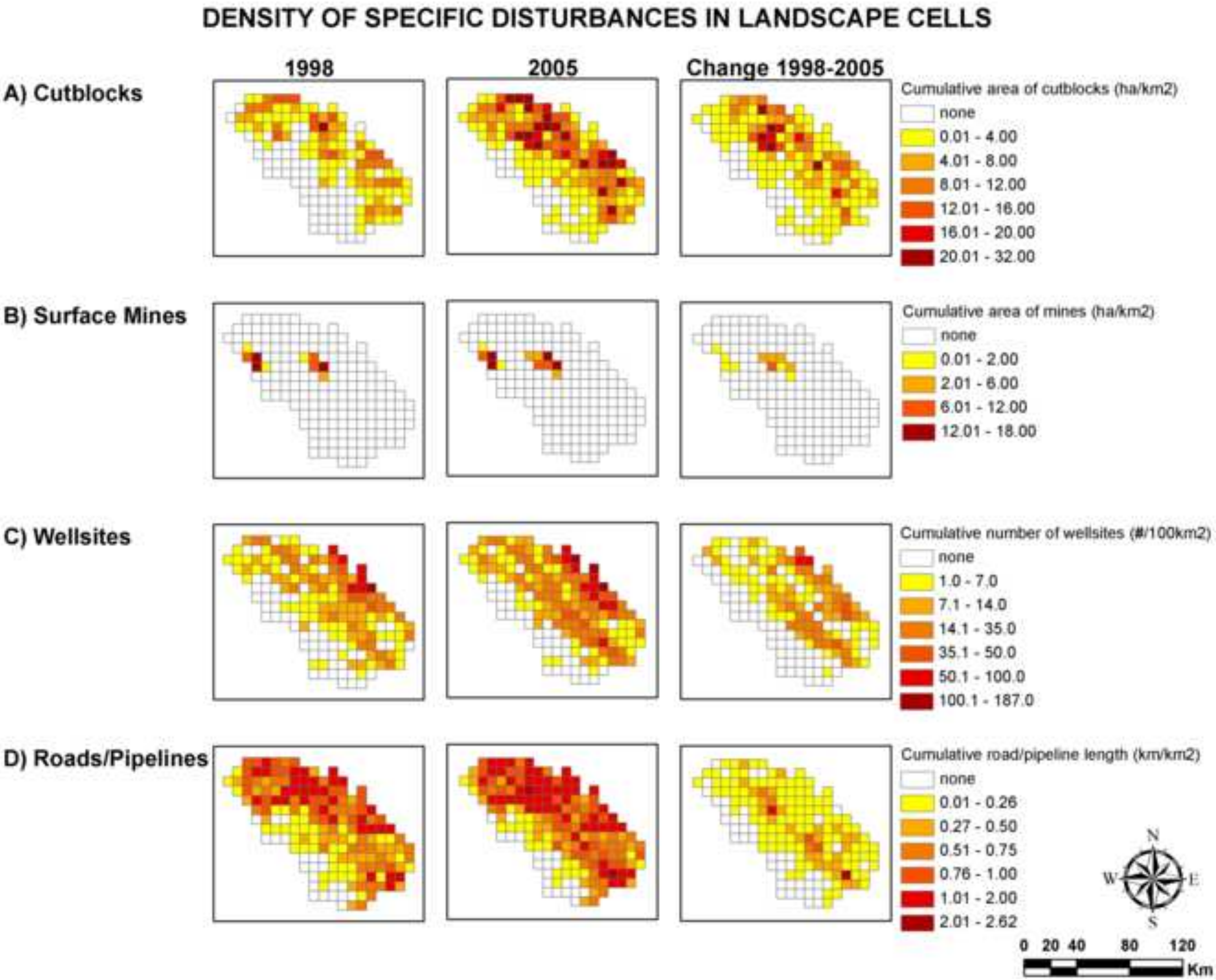

Figure 7
Click here to download high resolution image

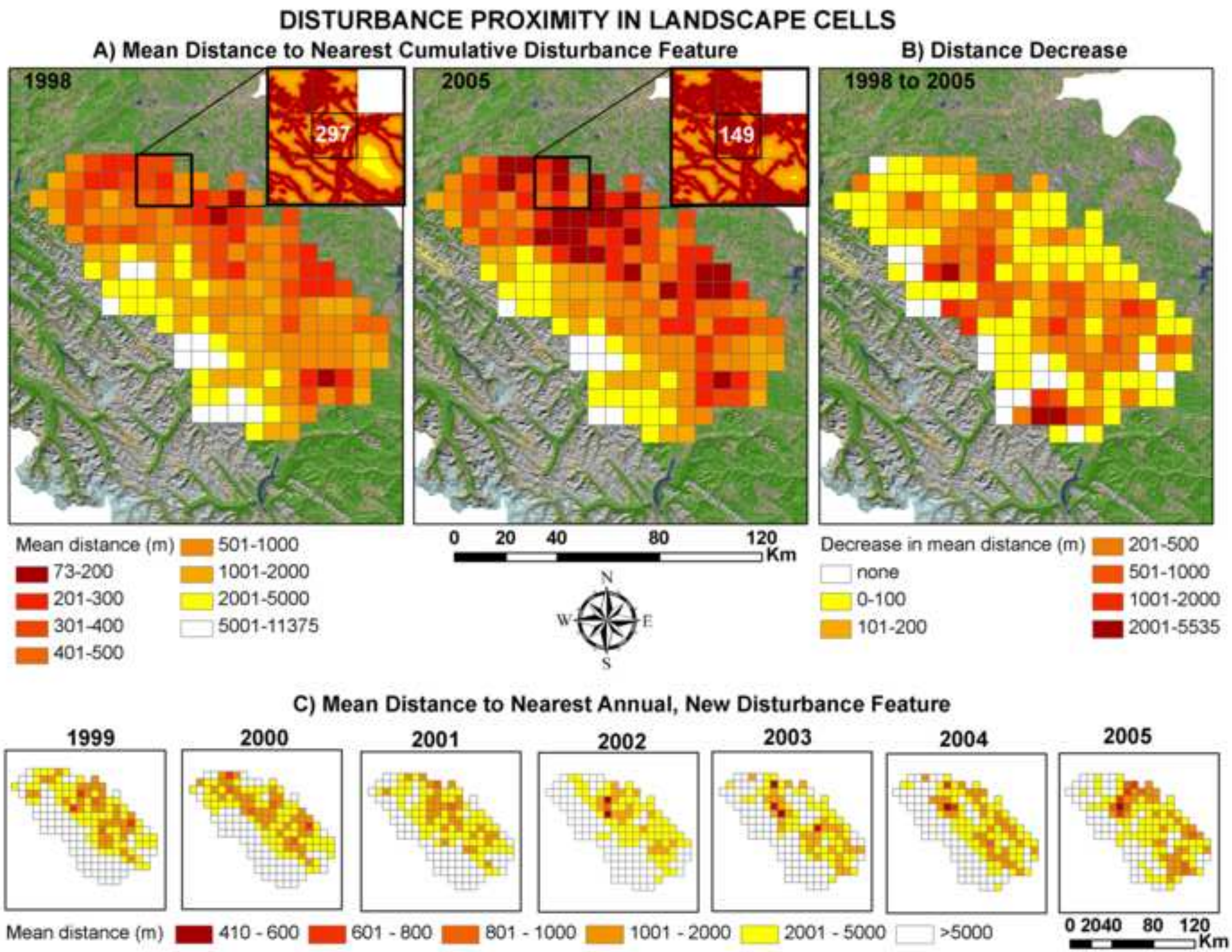

Figure 8
Click here to download high resolution image